PERGAMON

International Journal of Solids and Structures 37 (2000) 4577–4599

INTERNATIONAL JOURNAL OF SOLIDS and STRUCTURES

www.elsevier.com/locate/ijsolstr

Thermal stresses in a plate with a circular reinforcement

C.H. Wang*, L.R.F. Rose, R. Callinan, A.A. Baker

Aeronautical and Maritime Research Laboratory, Defence Science and Technology Organisation, P.O. Box 4331, Melbourne, Australia

Received 19 December 1998; in revised form 20 May 1999

Abstract

An analytical method is presented based on an inclusion analogy for determining the thermal residual stresses in an isotropic plate reinforced with a circular orthotropic patch. Explicit formulae are obtained for both the elastic properties and the thermal expansion coefficients of the equivalent inclusion. Exact solutions are derived for the thermal stresses in a circular orthotropic composite reinforcement bonded to an isotropic plate. To quantify the finite size effect, approximate solutions have also been obtained for a circular plate reinforced by a concentric circular patch. The present solutions are compared with finite element results, demonstrating a very good agreement with the numerical results. These explicit solutions provide a convenient tool for evaluating the residual thermal stresses when designing bonded repairs.

Keywords: Thermal stress; Composite stress; Elasticity; Stress analysis

1. Introduction

Bonded composite patch repair involves firstly heating the local area being patched above the ambient temperature, and subsequently cooling the fully cured patch, which can be regarded as rigidly bonded to the structure, to the ambient temperature. For instance, in a typical repair applied to aircraft structures the reinforced region is initially heated to a temperature of approximately 100–120°C, under pressure, for approximately one hour and then cooled down to the ambient temperature after the adhesive is cured (Baker, 1988; Rose, 1988). Due to the differences between the elastic properties and the thermal expansion properties of the composite patch and the metal plate, thermal residual stresses may arise. It has long been recognised that in some instances the thermal residual stresses represent a serious concern to the repair efficiency of composite patch repair. This is because the residual stresses in the metal plate

* Corresponding author. Tel.: +61-3-9626-7125; fax: +61-3-9626-7089.
E-mail address: chun-hui.wang@dsto.defence.gov.au (C.H. Wang).

0020-7683/00/$ - see front matter
PII: S0020-7683(99)00175-4

are almost inevitably tensile owing to the lower thermal expansion coefficient of the composite patch. In the case of crack patching, where a composite patch is bonded to a cracked structure, this tensile residual stress would translate into a positive mean stress-intensity factor, promoting faster crack growth.

Due to the complexity of the problem of analysing the cooling of fully cured patch subjected to the constraint of the surrounding material, studies to date have been concerned mainly with isotropic patches (Rose, 1988; Baker, 1988; Callinan et al., 1997). However, composite patches employed in repairing aircraft structures, such as unidirectional boron composite patches, are strongly orthotropic with vastly different elastic moduli and thermal expansion coefficients in different directions. Therefore, assuming the composite patch as an isotropic material may result in erroneous estimate of the thermal residual stresses.

The purpose of this article is to present a closed form solution for the thermal stresses resulting from the two steps of bonding a circular patch bonded on an infinite plate. The thermal stresses due to the first step (heating of the region to be repaired) can be readily determined using known results, which will be briefly outlined in Section 2. The emphasis of this article is on the thermal stresses induced by the second step: cooling of a plate reinforced with an orthotropic patch. The present analysis is facilitated by the known results of ellipsoidal inclusions (Eshelby, 1957). The problem is analysed with the help of imaginary cutting, straining and welding operations, in the spirit of the inclusion analogy by Eshelby (1957). The patched region (patch and plate) is modelled as an equivalent inclusion. The elastic properties and the thermal expansion coefficients of the equivalent inclusion are presented in Section 3.

To determine the thermal stresses developed in the patch and the plate, the patched region is first cut out from the plate, and then surface tractions of equal magnitude but opposite in sign are applied, respectively around the outer edge of the cut region and the hole in the plate. The unknown tractions are determined by closing the 'gap' between the patch and the hole; in doing so, continuity in both the tractions and displacement across the imaginary cut has to be satisfied simultaneously. As anticipated from the known results for the ellipsoidal inclusion, the stresses in the patch and the plate directly beneath the patch are uniform, provided that the temperature in the reinforced region is uniform. This special feature of ellipsoidal inclusions greatly simplifies the strategy for deriving an explicit solution; detailed derivations are presented in Section 4.

To quantify the finite size effect on the thermal stresses, an approximate solution is presented in Section 5, which is expected to provide good estimate of the thermal stresses in a circular plate reinforced with a concentric patch whose diameter is relatively smaller than that of the plate. The newly developed solutions have been validated using a finite element method. The main advantage of the present solutions over numerical methods such as the finite element method is the ability to account for the large number of parameters that affect the residual stresses. Therefore, the present solutions provide a convenient tool for the design and analysis of bonded repairs.

2. Problem description

The problem to be analysed can be idealised as a plate of uniform thickness $2t$, referring to Fig. 1, which is reinforced by two identical patches placed directly opposite one another across the plate, with one patch bonded to each face of the plate. The symmetry of this configuration ensures that no out-of-plane deflection will occur due to the thermal residual stresses. The issue of out-of-plane bending pertaining to one-sided repair will be addressed separately. To simplify the problem we can imagine the plate cut along its mid-plane and consider a plate of thickness t with a single reinforcement of thickness t_R bonded on one side. Following the usual conventions for bonded repairs, parameters pertaining to the reinforcement will be distinguished by a subscript or superscript R.

Consider the configuration shown in Fig. 1, in which a plate is reinforced by a circular patch of radius R_i. The coordinate system xy is chosen so that the principal axes of the orthotropic patch are aligned and parallel to the x-, y-axes, with the major direction along the x-axis. During the first step of bonding, suppose that the inner portion ($r < R_i$) is heated to a temperature T_i during the curing process, while the temperature at $r \geq R_o$ is heated to T_o, with the usual convention that the ambient temperature is taken as the zero of temperature. The temperature field satisfies the Laplacian equation,

$$\nabla^2 T = 0 \tag{1}$$

which has the following solution,

$$T^H(r) = \begin{cases} T_i & r < R_i \\ T_o + (T_i - T_o)\dfrac{\ln(r/R_o)}{\ln(R_i/R_o)} & R_i < r < R_o \\ T_o & R_o < r \end{cases} \tag{2}$$

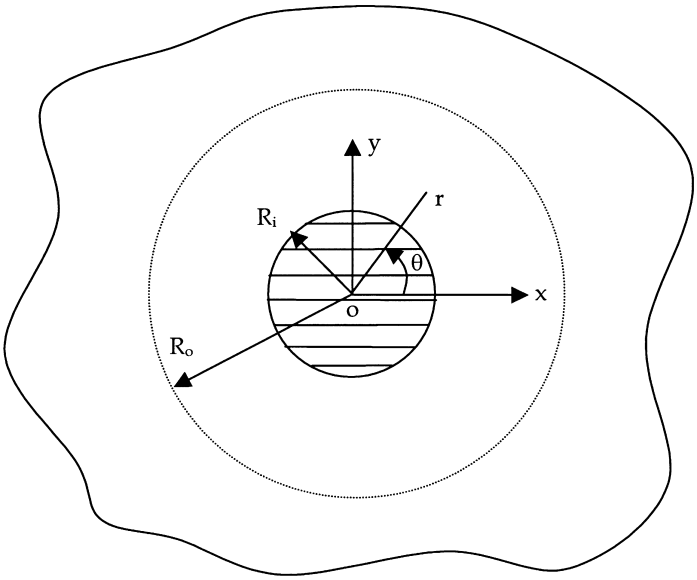

(a)

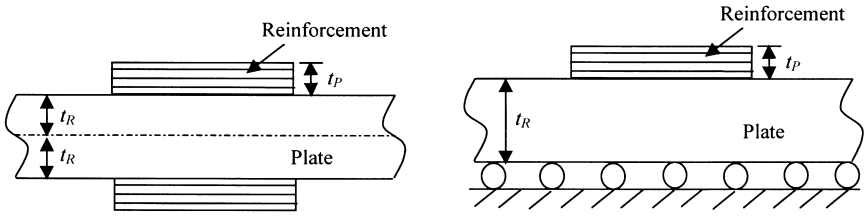

(b) (c)

Fig. 1. An infinite plate reinforced with a circular composite patch; (a) notations and coordinate, (b) cross-sectional view.

where the superscript H denotes the temperature change corresponding to the first step: heating. A schematic of the temperature distribution is shown in Fig. 2. Due to this non-uniform temperature distribution, thermal stresses develop in the plate, which can be readily derived (Timoshenko and Goodier, 1970, Section 150, pp. 441–443),

$$\sigma_{xx} = \sigma_{yy} = -\frac{1}{2}\alpha E(T_i - T_o) \tag{3}$$

where α and E denote the thermal expansion coefficient and Young's modulus of the plate. Since $T_i - T_o > 0$ during heating, the above thermal initial stress is compressive, as expected. It should be noted that this thermal stress arises only in the case of localised heating of a large structure; for the case of a finite size specimen being uniformly heated to T_i, no thermal stress will develop. This stress distribution serves as the initial stress that will be added to the thermal stress induced by cooling the patched region down to the ambient temperature.

For the second step of adhesive bonding we assume that there is no shear stress in the adhesive layer during curing, so that the reinforcing patch expands freely without developing any stresses. After the adhesive is fully cured, the patched plate is then cooled down to the ambient temperature. In other words, the temperature change over the entire patched plate is subjected to the following temperature field, referring to Fig. 2,

$$T^C(r) = -T^H(r) \tag{4}$$

where the superscript C denotes the temperature change corresponding to the second step: cooling. During this cooling process, it is assumed that the adhesive bond between the composite patch and the metal plate is absolutely rigid, so that the same strain state prevails in both the patch and the plate directly beneath the patch.

Due to anisotropy of the composite patch, the cooling step can no longer be modelled as an axisymmetric problem like in the case of an isotropic patch (Rose, 1988). However, in view of Eshelby's (Eshelby, 1957) results for ellipsoidal inclusions, it is reasonable to anticipate that the thermal stresses are uniform throughout the patched region, including the patch and the plate beneath the patch. Then this stress state can be determined with the help of a simple set of imaginary cutting, straining and welding operations, and by imposing requirements of traction and displacement continuity. The ability to satisfy these requirements confirms the correctness of the postulate of uniform stress.

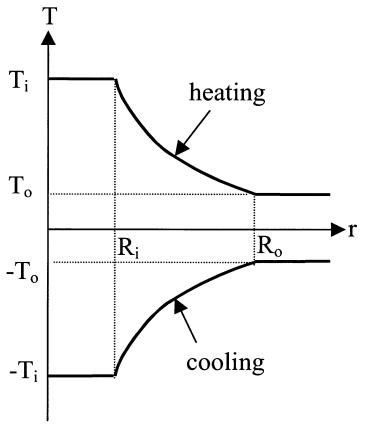

Fig. 2. Temperature distribution during heating and cooling.

3. Inclusion analogy

For convenience, the plate is divided into an inner region ($r < R_i$) lying under the reinforcement, and an outer region ($r > R_i$). The patch and the inner region of the plate are together called an 'inclusion'. In the following, the equivalent properties of the inclusion will be first determined so that the reinforced region can be replaced with an equivalent inclusion without altering the stress or displacement. Here and in the following the superscript I will be used to distinguish parameters pertaining to the inclusion.

Due to the expectation of uniform stress and the fact of symmetry with respect to the x- and y-axes, the shear stress τ_{xy} is zero everywhere within the patched region. This implies that the boundary tractions along the outer edge of the patched region is equivalent to a yet unknown but uniform stress-state of $\sigma_{xx} = p$ and $\sigma_{yy} = q$. The stress–strain relations for an orthotropic plate can be expressed as

$$\begin{Bmatrix} \varepsilon_{xx} \\ \varepsilon_{yy} \end{Bmatrix} = \begin{bmatrix} \dfrac{1}{E_1} & -\dfrac{\nu_{12}}{E_1} \\ -\dfrac{\nu_{21}}{E_2} & \dfrac{1}{E_2} \end{bmatrix} \begin{Bmatrix} \sigma_{xx} \\ \sigma_{yy} \end{Bmatrix} + \begin{Bmatrix} \alpha_1 \\ \alpha_2 \end{Bmatrix} T \tag{5}$$

where ε_{xx} and ε_{yy} denote the principal strain components, E_1 and E_2 the major Young's moduli, α_1 and α_2 the coefficients of thermal expansion, and the two Poisson's ratios, ν_{12} and ν_{21} are related by

$$\nu_{21} E_1 = \nu_{12} E_2 \tag{6}$$

The relationship given by Eq. (5) can be rewritten as

$$\begin{Bmatrix} \sigma_{xx} \\ \sigma_{yy} \end{Bmatrix} = [A] \begin{Bmatrix} \varepsilon_{xx} \\ \varepsilon_{yy} \end{Bmatrix} - [A] \begin{Bmatrix} \alpha_1 \\ \alpha_2 \end{Bmatrix} T \tag{7}$$

where the stiffness matrix A is given by,

$$[A] = \begin{bmatrix} \dfrac{E_1}{1-\nu_{12}\nu_{21}} & \dfrac{\nu_{12}E_2}{1-\nu_{12}\nu_{21}} \\ \dfrac{\nu_{12}E_2}{1-\nu_{12}\nu_{21}} & \dfrac{E_2}{1-\nu_{12}\nu_{21}} \end{bmatrix} \tag{8}$$

As shown in Fig. 3(a), the inclusion is subjected to the following uniform surface tractions

$$\left(F_x, F_y\right) = (px/R_i, qy/R_i) \tag{9}$$

The equations of equilibrium and strain compatibility can be expressed as

$$\sigma^{I}_{\alpha\beta} t_I = \sigma_{\alpha\beta} t + \sigma^{R}_{\alpha\beta} t_R \tag{10}$$

$$\varepsilon^{I}_{\alpha\beta} = \varepsilon_{\alpha\beta} = \varepsilon^{R}_{\alpha\beta} \tag{11}$$

where the Greek subscripts α and β stand for x or y, and parameters pertaining to the reinforcement and the inclusion are distinguished, respectively, by subscript or superscript R and I; symbols carrying no such label pertain to the plate. The inclusion thickness t_I can be chosen arbitrarily, but it will prove advantageous in the present context to choose

$$t_{\mathrm{I}} = t \tag{12}$$

so that the force continuity given by Eq. (16) becomes stress continuity (Rose, 1981).

Since Eq. (10) must hold for arbitrary ε_{xx}, ε_{yy} and T, the following relations can be obtained

$$[A^{\mathrm{I}}] = [A] + \frac{t_{\mathrm{R}}}{t}[A^{\mathrm{R}}] \tag{13}$$

$$\begin{Bmatrix} \alpha_1^{\mathrm{I}} \\ \alpha_2^{\mathrm{I}} \end{Bmatrix} = [C^{\mathrm{I}}][A]\begin{Bmatrix} \alpha_1 \\ \alpha_2 \end{Bmatrix} + \frac{t_{\mathrm{R}}}{t}[C^{\mathrm{I}}][A^{\mathrm{R}}]\begin{Bmatrix} \alpha_1^{\mathrm{R}} \\ \alpha_2^{\mathrm{R}} \end{Bmatrix} \tag{14}$$

where

$$[C^{\mathrm{I}}] = [A^{\mathrm{I}}]^{-1} \equiv \begin{bmatrix} \dfrac{1}{E_1^{\mathrm{I}}} & \dfrac{-\nu_{12}^{\mathrm{I}}}{E_1^{\mathrm{I}}} \\ \dfrac{-\nu_{21}^{\mathrm{I}}}{E_2^{\mathrm{I}}} & \dfrac{1}{E_2^{\mathrm{I}}} \end{bmatrix} \tag{15}$$

It is seen that the stiffness of the equivalent inclusion is identical to that obtained by Rose (1981). It is interesting to note that, however, the thermal expansion coefficients of the equivalent inclusion depend on the stiffness of the reinforcement and the plate, in addition to the respective expansion coefficients.

4. Infinite plate reinforced with a circular patch

Having determined the elastic properties and the thermal expansion coefficients of the equivalent inclusion, we can now analyse the thermal stresses in a circular patch bonded on to an infinite plate. To do this, the inclusion is first cut out from the plate and unknown tractions are applied to the outer edge of the inclusion and the boundary of the hole. The purpose of this boundary traction is to close the 'gap' between the hole and the inclusion.

Assuming that the reinforced region can be replaced with an equivalent inclusion without altering the stress or displacement both in the inner region and the outer region, the problem reduces to finding the stresses being transmitted across the inclusion/plate interface. Evidently the continuity of (a) the tractions across the inclusion/plate interface and (b) the displacement along the interface must be maintained. Mathematically these two conditions can be expressed as (Rose, 1981)

$$F_\alpha^{\mathrm{I}}\left(r \to R_{\mathrm{i}}^-\right) = F_\alpha\left(r \to R_{\mathrm{i}}^+\right) \tag{16}$$

$$u_\alpha^{\mathrm{I}}\left(r \to R_{\mathrm{i}}^-\right) = u_\alpha\left(r \to R_{\mathrm{i}}^+\right) \tag{17}$$

where the traction F_α is defined as $F_\alpha = -t\sigma_{\alpha\beta}n_\beta$ and $\sigma_{\alpha\beta}$ (Greek subscripts α and β stand for x and y) denote the stresses, and $n_\alpha = (x/R_{\mathrm{i}}, y/R_{\mathrm{i}})$ denote the components of the outward vector normal to the inclusion boundary. The usual convention that repeated Greek subscripts imply a summation applies. Because the displacement u_α^{I} and u_α are dependent on the surface tractions across the inclusion/plate interface, the two equations (16) and (17) are coupled. However, as will be shown later, a unique solution of the surface tractions can be derived which satisfy exactly the above conditions of force and displacement continuity.

To perform the matching of the displacements across the interface between the inclusion and the

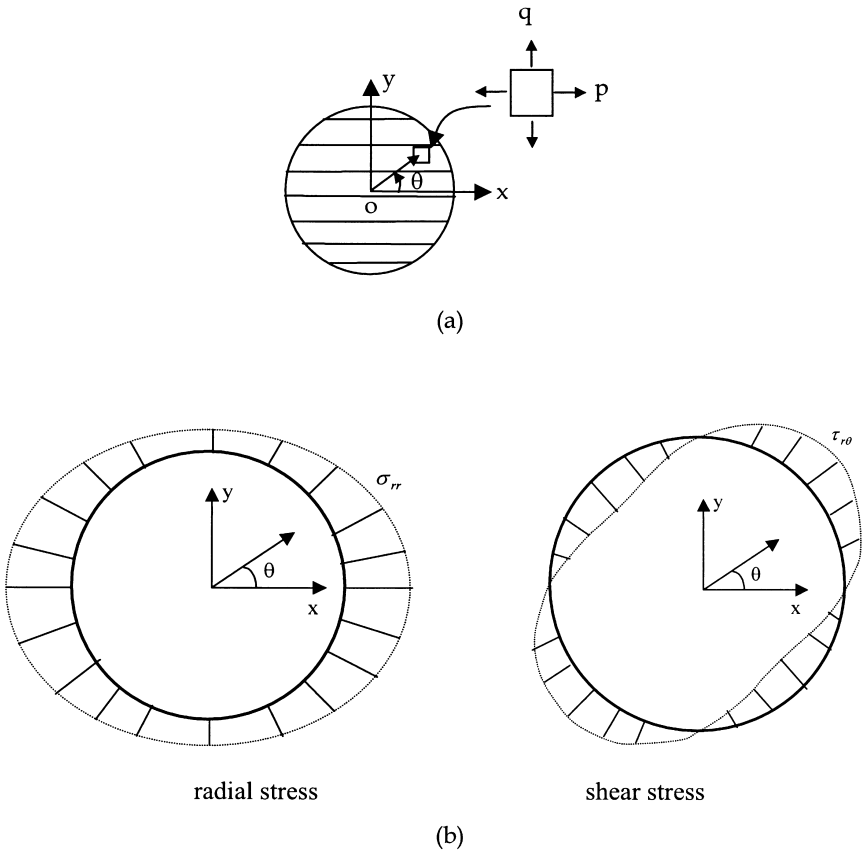

Fig. 3. Loading on the equivalent inclusion and the circular hole; (a) inclusion in a uniform stress state, (b) a circular hole subjected to internal surface loading.

plate, the solutions of three sub-problems are required. These are the solutions corresponding to (1) circular orthotropic inclusion subjected to a boundary traction and uniform temperature change, (2) a plate with a circular hole subjected to internal surface traction and (3) a plate with a circular hole subjected to non-uniform temperature change given by Eq. (4).

4.1. Orthotropic inclusion subjected to traction and temperature loading

Referring to Fig. 3(a), the displacements at a generic point (x, y) on the boundary of the inclusion that is subjected to the surface tractions given by Eq. (9) and a uniform temperature change of $-T_i$ are

$$\begin{Bmatrix} u_x^I \\ u_y^I \end{Bmatrix} = \begin{Bmatrix} \varepsilon_{xx}^I x \\ \varepsilon_{yy}^I y \end{Bmatrix} \tag{18}$$

where

$$\begin{Bmatrix} \varepsilon_{xx}^I \\ \varepsilon_{yy}^I \end{Bmatrix} = [C^I] \begin{Bmatrix} p \\ q \end{Bmatrix} + \begin{Bmatrix} \alpha_1^I \\ \alpha_2^I \end{Bmatrix} (-T_i) \tag{19}$$

It can be seen that the displacement components u_x and u_y are, respectively, proportional to the coordinate x or y, corresponding to a uniform strain field. As will be seen later, this feature is essential to the matching of the displacement along the interface between the inclusion and the plate.

4.2. Internal loading of a circular hole in an infinite plate

This sub-problem is that of a circular hole in an infinite plate subjected to the following internal loading along the hole boundary,

$$\sigma_{rr} - i\tau_{r\theta} = \frac{p+q}{2} + \frac{p-q}{2}\mathrm{e}^{2i\theta} \tag{20}$$

where i represents $\sqrt{-1}$. The radial and shear tractions are illustrated in Fig. 3(b) and (c). The non-uniform nature of the boundary conditions means that the problem is not axisymmetric. To solve this problem, we will adopt the complex potential method of Muskhelishvili (1953). Stresses and displacements are expressed in terms of two complex potentials, ϕ and ψ,

$$\sigma_{xx} + \sigma_{yy} = 4\mathrm{Re}\left[\phi'\right] \tag{21}$$

$$\sigma_{yy} - \sigma_{xx} + i2\tau_{xy} = 2\left(\bar{z}\phi'' + \psi'\right) \tag{22}$$

$$2\mu\left(u_x + iu_y\right) = \frac{3-\nu}{1+\nu}\phi - z\bar{\phi}' - \bar{\psi} \tag{23}$$

Writing $\chi = \mathrm{e}^{i\theta}$, the boundary condition (20) becomes,

$$\phi(\chi) + \chi\bar{\phi}'(\bar{\chi}) + \bar{\psi}(\bar{\chi}) = f(\chi) \tag{24}$$

where the forcing term $f(\chi)$ can be obtained by integration,

$$f(\chi) = R_\mathrm{i}\left[\frac{p}{2}\left(\chi + \chi^{-1}\right) + \frac{q}{2}\left(\chi - \chi^{-1}\right)\right] \tag{25}$$

The expressions for the two complex potentials can now be derived using the contour integral method (Timoshenko and Goodier, 1970, pp. 206–214). Omitting the details of derivation, the complex potentials are,

$$\phi(z) = \frac{R_\mathrm{i}^2}{2z}(q-p) \tag{26}$$

$$\psi(z) = \frac{R_i^2}{2z}\left[(p+q) + \frac{R_i^2}{z^2}(q-p)\right] \tag{27}$$

Consequently, the displacements at a generic point along the hole boundary become, noting that $x = R_\mathrm{i}\cos\theta$, $y = R_\mathrm{i}\sin\theta$,

$$u_x^{pq} = -\frac{x}{E}\left[2p - (1-\nu)q\right] \tag{28a}$$

$$u_y^{pq} = -\frac{y}{E}\left[2q - (1-\nu)p\right] \tag{28b}$$

where the superscript pq is used to distinguish the displacement induced by the surface traction given by Eq. (20). Again, it is noted that the displacement components u_x and u_y are, respectively, proportional to the coordinate x or y.

4.3. Steady-state thermal analysis of an infinite plate with a circular hole

The third sub-problem is to determine the displacement field in an infinite plate containing a hole that is subjected to the non-uniform temperature change given by Eq. (4). As expected, due to the non-uniform temperature distribution outside the hole, stresses and displacement will develop in the plate. Since the temperature field is axisymmetric, the analysis can be considerably simplified. In particular, the general solutions of the radial displacement and the radial stress can be expressed as (Timoshenko and Goodier, 1970),

$$u_r^{\mathrm{C}}(r) = \frac{(1+\nu)\alpha}{r}\int_{R_\mathrm{i}}^{r} T(r) r \,\mathrm{d}r + c_1 r + \frac{c_2}{r} \tag{29}$$

$$\sigma_{rr}^{\mathrm{C}}(r) = -\frac{E\alpha}{r^2}\int_{R_\mathrm{i}}^{r} T(r) r \,\mathrm{d}r + \frac{E}{1-\nu^2}\left[c_1(1+\nu) - \frac{c_2(1-\nu)}{r^2}\right] \tag{30}$$

where the superscript C is used to denote the displacement induced by cooling. The temperature $T(r)$ is given by Eq. (4). The two parameters, c_1 and c_2, are integration constants yet to be determined from the following boundary conditions,

$$\sigma_{rr}(r = R_\mathrm{i}) = 0 \tag{31}$$

$$\sigma_{rr}(r \to \infty) = 0 \tag{32}$$

from which the two integral constants c_1 and c_2 can be obtained,

$$c_1 = -\frac{1-\nu}{2}\alpha T_\mathrm{o} \tag{33}$$

$$c_2 = -\frac{1+\nu}{2}\alpha T_\mathrm{o} R_\mathrm{i}^2 \tag{34}$$

Therefore, the radial displacement at the inner radius can be expressed as

$$u_r^{\mathrm{C}} = -\omega T_\mathrm{i} R_\mathrm{i}, \quad T_\mathrm{i} > 0 \tag{35}$$

where $\omega = \alpha T_\mathrm{o}/T_\mathrm{i}$. Consequently, the x- and y-displacement components are

$$\begin{Bmatrix} u_x^{\mathrm{C}} \\ u_y^{\mathrm{C}} \end{Bmatrix} = -\omega T_\mathrm{i} \begin{Bmatrix} x \\ y \end{Bmatrix} \tag{36}$$

It can be seen that the displacement components u_x and u_y are, respectively, proportional to the coordinate x or y, exhibiting the same behaviour as the displacements in the equivalent inclusion and

the displacements corresponding to the internally loaded hole. Consequently, an exact matching in displacements across the inclusion/plate interface can now be guaranteed.

4.4. Thermal residual stresses

With the solutions of the above three sub-problems being fully determined, we can now proceed to perform the displacement matching, as the condition of force continuity (16) is already satisfied. The displacement continuity (17) can now be expressed as

$$\begin{Bmatrix} u_x^{\mathrm{I}} \\ u_y^{\mathrm{I}} \end{Bmatrix} = \begin{Bmatrix} u_x^{pq} \\ u_y^{pq} \end{Bmatrix} + \begin{Bmatrix} u_x^{\mathrm{C}} \\ u_y^{\mathrm{C}} \end{Bmatrix} \tag{37}$$

which yields, noting Eqs. (18), (28a), (28b) and (36)

$$pB_{11} + qB_{12} + \left(\alpha_1^{\mathrm{I}} - \omega\right)(-T_{\mathrm{i}}) = 0 \tag{38a}$$

$$pB_{21} + qB_{22} + \left(\alpha_2^{\mathrm{I}} - \omega\right)(-T_{\mathrm{i}}) = 0 \tag{38b}$$

where

$$B_{11} = \frac{1}{E_1^{\mathrm{I}}} + \frac{2}{E} \tag{39a}$$

$$B_{12} = B_{21} = -\frac{\nu_{12}^{\mathrm{I}}}{E_1^{\mathrm{I}}} - \frac{1-\nu}{E} \tag{39b}$$

$$B_{22} = \frac{1}{E_2^{\mathrm{I}}} + \frac{2}{E} \tag{39c}$$

Consequently, the unknown inclusion stresses p and q are given by

$$p = \frac{\left(\alpha_1^{\mathrm{I}} - \omega\right)B_{22} - \left(\alpha_2^{\mathrm{I}} - \omega\right)B_{12}}{B_{11}B_{22} - (B_{12})^2} T_{\mathrm{i}} \tag{40a}$$

$$q = \frac{\left(\alpha_2^{\mathrm{I}} - \omega\right)B_{11} - \left(\alpha_1^{\mathrm{I}} - \omega\right)B_{21}}{B_{11}B_{22} - (B_{12})^2} T_{\mathrm{i}} \tag{40b}$$

With the strains in the reinforcement and the plate being equal to the strain in the inclusion, which is given by Eq. (19), the stresses in the reinforcement and the plate lying under the reinforcement can be evaluated by

$$\begin{Bmatrix} \sigma_{xx} \\ \sigma_{yy} \end{Bmatrix} = [A] \begin{Bmatrix} \varepsilon_{xx}^{\mathrm{I}} + \alpha T_{\mathrm{i}} \\ \varepsilon_{yy}^{\mathrm{I}} + \alpha T_{\mathrm{i}} \end{Bmatrix} \tag{41}$$

$$\begin{Bmatrix} \sigma_{xx}^{R} \\ \sigma_{yy}^{R} \end{Bmatrix} = [A^{R}] \begin{Bmatrix} \varepsilon_{xx}^{I} + \alpha_1^{R} T_i \\ \varepsilon_{yy}^{I} + \alpha_2^{R} T_i \end{Bmatrix} \tag{42}$$

This furnishes the exact solutions of the thermal stresses in the both the plate and the reinforcement. Validity of the present theory will be demonstrated in Section 6 by comparing with detailed finite element results obtained for a typical reinforcement over an isotropic plate.

5. Influence of finite size

The solution presented in the previous section applies strictly for an infinite plate. In practice, however, structures to be reinforced may be finite in size. For instance, the size of representative specimens that are widely used in laboratory studies (Baker, 1988) is often comparable to the size of the reinforcement. In this case, the previous solutions may need to be modified to incorporate the size effect on the residual thermal stress.

Due to the finite size of the plate, the stresses in the inclusion are no longer uniform. Although the problem could be formulated using the 'stretched coordinate' method by Lekhnitskii (1963), the analysis becomes rather unwieldy, as the solutions need to be represented by infinite series. For simplicity, here we will present an approximate solution, whose accuracy will be assessed both analytically and by comparing with finite element results.

It will prove useful to consider the problem of circular patch on a concentric circular plate, as shown in Fig. 4. For simplicity, let us assume that the annulus is constrained at radius R_o by a continuous distribution of springs according to the following relation,

$$\sigma_{rr}(r = R_o) = -kEu_r(r = R_o) \tag{43}$$

It can be shown from Eqs. (28a) and (28b) that with the following spring stiffness k, the infinite plate can be recovered as a special case,

$$k = \frac{1}{(1+\nu)R_o} \tag{44}$$

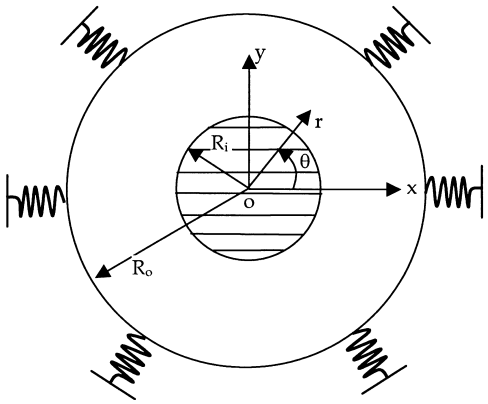

Fig. 4. Spring representation for simulating finite size effect.

Furthermore, the cases of free edge and a clamped edge $r = R_o$ can be recovered by setting $k = 0$ and $k \to \infty$, respectively.

While the properties of the equivalent inclusion remain the same as those obtained in Section 3, the solutions pertaining to the thermal loading and the internal loading need to be modified to account for the finite size effect. In this case, the two auxiliary sub- problems need to be re-analysed to take into account of the finite size.

5.1. Internally loaded annulus

Let us consider an annulus with an inner radius and outer radius of R_i and R_o, respectively. The annulus is loaded at its inner radius by the surface traction (Eq. (20)) while its outer radius is constrained. To facilitate the following analysis, the surface loading is decomposed into a uniform radial loading and a 'shear' loading,

$$\sigma_{rr} - i\tau_{r\theta} = \frac{p+q}{2} \tag{45}$$

$$\sigma_{rr} - i\tau_{r\theta} = \frac{p-q}{2} e^{2i\theta} \tag{46}$$

The first component represents a uniform radial pressure on the hole, whereas the second mode represents a shear stress state: $\sigma_{xx} = -\sigma_{yy} = (p-q)/2$. Due to the axisymmetric nature of the uniform radial loading, a closed-form solution can be derived (details shown below). The 'shear' loading problem can be analysed by expanding the complex potentials in a Laurent series (Muskhelishvili, 1953, pp. 218–223).

The problem of an annulus with constraint along its outer edge and subjected to a uniform radial pressure on its inner edge can be analysed using the known results (Timoshenko and Goodier, 1970). The appropriate boundary conditions are

$$\sigma_{rr}(r = R_i) = \frac{(p+q)}{2} \tag{47}$$

$$\sigma_{rr}(r = R_o) = -kEu_r(r = R_o) \tag{48}$$

After some algebra manipulations, the following solution can be derived for displacement at the inner edge of the hole,

$$u_r(r = R_i) = -\frac{p+q}{2}\frac{(1+\nu)R_i}{E}\lambda \tag{49}$$

where

$$\lambda = \frac{1+\nu+\beta(1-\nu)R_i^2/R_o^2}{(1+\nu)(1-\beta R_i^2/R_o^2)}, \quad \beta = \frac{1-(1+\nu)kR_o}{1+(1-\nu)kR_o} \tag{50}$$

To analyse the problem of an annulus subjected to the surface traction (Eq. (46)) on its inner radius, the boundary condition is written in terms of complex Fourier series,

$$\sigma_{rr} - i\tau_{r\theta} = \sum_{-\infty}^{\infty} A_k e^{ik\theta} \tag{51}$$

Comparing with Eq. (46), we have

$$A_k = \begin{cases} \dfrac{p-q}{2} & k=2 \\ 0 & k\neq 2 \end{cases}. \tag{52}$$

The two complex potentials $\phi(z)$ and $\psi(z)$ are expanded in terms of Laurent series,

$$\phi(z) = \sum_{-\infty}^{\infty} \frac{a_k}{k+1} z^{k+1} \tag{53}$$

$$\psi(z) = \sum_{-\infty}^{\infty} \frac{b_k}{k+1} z^{k+1} \tag{54}$$

According to Muskhelishvili (1953), the coefficients a_k and b_k can be determined as following:

$$a_k = \begin{cases} \dfrac{R_o^6 - R_i^6}{3\left(R_o^2 - R_i^2\right)^2 + \left(R_o^6 - R_i^6\right)\left(R_o^{-2} - R_i^{-2}\right)} \bar{B}_2, & k=-2 \\ -\dfrac{3\left(R_o^2 - R_i^2\right)}{3\left(R_o^2 - R_i^2\right)^2 + \left(R_o^6 - R_i^6\right)\left(R_o^{-2} - R_i^{-2}\right)} B_2, & k=2 \\ 0, & k\neq -2,2 \end{cases} \tag{55}$$

$$b_k = \begin{cases} 3a_{-2}R_i^2 + a_2 R_i^6, & k=-4 \\ \bar{a}_{-2}R_i^{-2} - a_2 R_i^2 - A_2, & k=0 \\ 0, & k\neq -4, 0 \end{cases} \tag{56}$$

$$B_2 = \bar{B}_2 = -\frac{p-q}{2} \tag{57}$$

Therefore, the complex potentials become

$$\phi(z) = -\frac{a_{-2}}{z} + \frac{a_2 z^3}{3} \tag{58}$$

$$\psi(z) = b_0 z - \frac{b_{-4}}{3z^3} \tag{59}$$

According to Eq. (23), the displacements at the inner radius $r = R_i$ are (using Eq. (6)),

$$u_x^{p-q} + i u_y^{p-q} = -\frac{p-q}{2}\frac{3-\nu}{E}\eta R_i\left[e^{-i\theta} - \rho e^{3i\theta}\right] \tag{60}$$

where the superscript $p-q$ is used to denote displacement components pertaining to the 'shear' loading, and

$$\eta = \frac{3-\nu+(7+3\nu)R_i^2/R_o^2+(1-3\nu)R_i^4/R_o^4+(1+\nu)R_i^6/R_o^6}{(3-\nu)\left(1-R_i^2/R_o^2\right)^3} \tag{61}$$

$$\rho = \frac{3(1+\nu)\left(1-R_i^2/R_o^2\right)R_i^4/R_o^4}{(3-\nu)\eta\left[1-4R_i^2/R_o^2+6R_i^4/R_o^4-4R_i^6/R_o^6+R_i^8/R_o^8\right]} \tag{62}$$

It is worth noting that, due to the presence of $e^{3i\theta}$ in Eq. (60), the displacements are no longer proportional to the coordinates x and y. This implies that the postulation of a uniform stress state in the inclusion will no longer satisfy the displacement continuity condition at the inclusion/plate interface, for the displacements at the hole radius induced by the temperature change (detailed later) are proportional to the coordinates x and y. Therefore, strictly speaking, the most important feature of ellipsoidal inclusion that the stresses being uniform inside the inclusion is lost, due to the finite size of the plate. Exact solutions of the problem would then become unwieldy, involving the analysis of an orthotropic disk subjected to non-uniform surface tractions.

Nevertheless, it is interesting to observe that the parameter ρ in Eq. (60) is generally very small provided that the outer radius of the annulus is reasonably greater than its inner radius. A graphical representation of the parameter ρ plotted against the ratio of outer radius to inner radius is shown in Fig. 5, which is indicative of the error associated with neglecting the higher order term. Maximum error occurs in the limiting case when R_o approaches R_i, i.e., when the width of the annulus approaches zero. Even in this case, the parameter ρ approaches the following limit,

$$\lim_{R_o \to R_i} \rho = \frac{1+\nu}{4} \tag{63}$$

It is also clear from Fig. 5 that provided the outer radius of the plate is moderately greater than the patch size, i.e., $R_o/R_i \geq 3$, the error incurred by dropping the higher order term $e^{3i\theta}$ from Eq. (60) will indeed be very small (less than 1%). Furthermore, since the displacement due to 'shear' loading solution forms only part of the total displacement, the overall error would be even smaller.

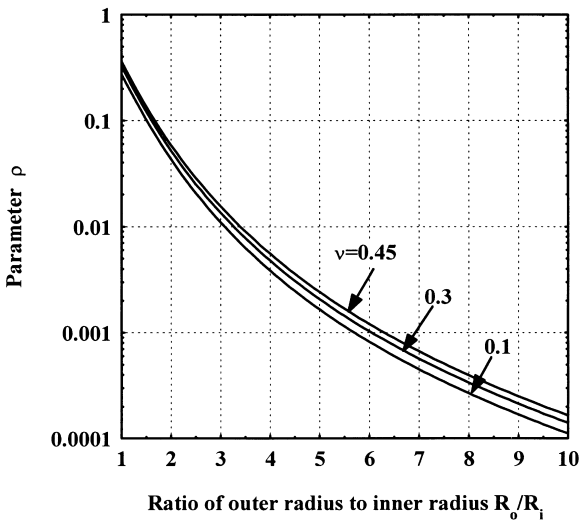

Fig. 5. Effect of annulus size on the displacement at inner radius due to 'shear' loading.

By neglecting the higher order term, approximate solutions of the total displacement at the inner radius of the annulus can be obtained by combining Eqs. (49) and (60), yielding,

$$\begin{Bmatrix} u_x^{pq} \\ u_y^{pq} \end{Bmatrix} = \begin{Bmatrix} -\dfrac{x}{E}(\gamma_1 p - \gamma_2 q) \\ -\dfrac{y}{E}(-\gamma_2 p + \gamma_1 q) \end{Bmatrix} \tag{64}$$

where

$$\gamma_1 = \frac{(3-\nu)\eta + (1+\nu)\lambda}{2} \tag{65}$$

$$\gamma_2 = \frac{(3-\nu)\eta - (1+\nu)\lambda}{2} \tag{66}$$

In the limiting case that the outer radius of the annulus is far greater than the inner radius, i.e., $R_i/R_o \to 0$, it is easy to verify that both η and λ approach unity. Consequently, the above solution recovers, as a special case, that corresponding to the internally loaded hole in an infinite plate (see Eqs. (28a) and (28b)).

5.2. Thermal loading of an annulus

The second sub-problem to be analysed is the displacement field in an annulus due to a steady-state, non-uniform, temperature change described by Eq. (4). Much of the method outlined in Section 4.2 can be followed, except that the relevant boundary conditions in the present case are,

$$\sigma_{rr} = 0, \quad r = R_i \tag{67}$$

$$\sigma_{rr} = -kEu_r, \quad r = R_o \tag{68}$$

After some lengthy algebra, the displacement at the inner radius is determined,

$$u_r(r = R_i) = -eT_i R_i \tag{69}$$

where

$$e = \frac{\alpha\beta}{1 - \beta R_i^2/R_o^2}\left\{ T_o/T_i - R_i^2/R_o^2 - \frac{(1 - R_i^2/R_o^2)(1 - T_o/T_i)}{2\ln(R_i/R_o)} \right\} \tag{70}$$

with

$$\beta = \frac{1 - (1+\nu)kR_o}{1 + (1-\nu)kR_o} \tag{71}$$

Therefore, the displacement at a generic point (x, y) on the hole edge due to the non-uniform thermal loading is

$$\begin{Bmatrix} u_x^T \\ u_y^T \end{Bmatrix} = -\begin{Bmatrix} x \\ y \end{Bmatrix} eT_i \tag{72}$$

As expected, both the displacement x- and y-displacements are proportional to the coordinates x and y. It can be shown that the following condition holds, provided that k is given by Eq. (44),

$$\lim_{R_i/R_o \to 0} e = 0 \tag{73}$$

which confirms that the above solution recovers, as a special case, that corresponding to an infinite plate with $T_o/T_i = 0$.

5.3. Thermal stresses

Having solved the two sub-problems, we can now perform the displacement matching to determine the unknown boundary tractions p and q. The condition of displacement continuity becomes,

$$\begin{Bmatrix} u_x^I \\ u_y^I \end{Bmatrix} = \begin{Bmatrix} u_x^{pq} \\ u_y^{pq} \end{Bmatrix} + \begin{Bmatrix} u_x^C \\ u_y^C \end{Bmatrix} \tag{74}$$

which leads to

$$pD_{11} + qD_{12} + \left(\alpha_1^I - e\right)(-T_i) = 0 \tag{75a}$$

$$pD_{21} + qD_{22} + \left(\alpha_2^I - e\right)(-T_i) = 0 \tag{75b}$$

where

$$D_{11} = \frac{1}{E_1^I} + \frac{\gamma_1}{E} \tag{76a}$$

$$D_{12} = D_{21} = -\frac{\nu_{12}^I}{E_1^I} - \frac{\gamma_2}{E} \tag{76b}$$

$$D_{22} = \frac{1}{E_2^I} + \frac{\gamma_1}{E} \tag{76c}$$

Therefore,

$$p = \frac{\left(\alpha_1^I - e\right)D_{22} - \left(\alpha_2^I - e\right)D_{12}}{D_{11}D_{22} - (D_{12})^2} T_i \tag{77a}$$

$$q = \frac{\left(\alpha_2^I - e\right)D_{11} - \left(\alpha_1^I - e\right)D_{21}}{D_{11}D_{22} - (D_{12})^2} T_i \tag{77b}$$

which furnishes the solutions for the unknown tractions p and q. The strains in the inclusion can be obtained by Eq. (19), and the stresses in the reinforcement and the plate are given by Eqs. (41) and (42).

Table 1
Properties and dimensions of isotropic reinforcement

Material	Young's modulus (GPa)	Poisson's ratio	Thickness (mm)	Thermal coefficient
Plate	71	0.3	1.0	23×10^{-6}
Reinforcement	156	0.3	0.5	6.24×10^{-6}

6. Comparison with finite element results

To validate the present theory and to examine the accuracy of the approximate solution for finite size plate, a detailed finite element analysis is carried out for both an isotropic patch and an orthotropic patch, simulating a cross-ply laminate composite patch. The properties and dimensions of the isotropic patch and the orthotropic patch are summarised in Tables 1 and 2. The ratios of the outer radius to inner radius, R_o/R_i, will be varied to investigate the size effect.

An example of finite element mesh employed is shown in Fig. 6. Due to symmetry, only a quarter of the problem is modelled using eight node quadrilateral elements, using the generalised plane stress formulation. With the reinforced region, elements pertaining to the patch and the plate share the same set of nodes, simulating a rigid bond between the reinforcement and the plate. Since the thermal stress due to the initial heating of the reinforcement region is well known, emphasis will be placed on the second step of adhesive bonding: cooling of the cured patch. The superposition of stresses determined from these two steps will yield the final residual thermal stresses in the plate and the reinforcement. The temperature distribution for the cooling is prescribed according to Eq. (4). As shown in Fig. 7, in the case of isotropic reinforcement, the closed-form solution is in excellent agreement with the finite element results. In fact, the difference between the analytical solutions and the finite element results is less than 0.1% for cases being examined.

To examine the influences of finite size on the uniformity of the strains within the reinforced region, strain distributions corresponding to the case of a circular orthotropic reinforcement over a circular plate are shown in Fig. 8. The outer edge of the plate is clamped and the ratio R_o/R_i is equal to 2. Despite the finite size effect, the strains within the reinforced region are nearly constant. Results corresponding to greater values of R_o/R_i, although not shown here for brevity, confirm that the uniformity of the strains within the reinforced region increases as R_o/R_i increases.

For a typical orthotropic reinforcement whose properties and dimensions are listed in Table 2, comparison of the stresses in the plate and the reinforcement as obtained using the finite element method and the present solutions are shown in Fig. 9. As in the case of isotropic reinforcement, there is a very good agreement between the analytical solution and the finite element results for all the cases being investigated. For comparison purposes, the predictions based on an equivalent isotropic reinforcement, which takes the major properties of the orthotropic reinforcement, are also shown in Fig. 9.

It can be shown that for the special case of isotropic patch, the residual thermal stress simplifies to

Table 2
Properties and dimensions of orthotropic reinforcement

Material	Young's modulus (GPa)	Poisson's ratio	Thickness (mm)	Thermal coefficient
Plate	71	0.3	3.0	23×10^{-6}
Reinforcement	$E_1 = 156$, $E_2 = 29.7$	$\nu_{21} = 0.1097$, $\nu_{12} = 0.5762$	1.5	$\alpha_1 = 6.24 \times 10^{-6}$, $\alpha_2 = 16.96 \times 10^{-6}$

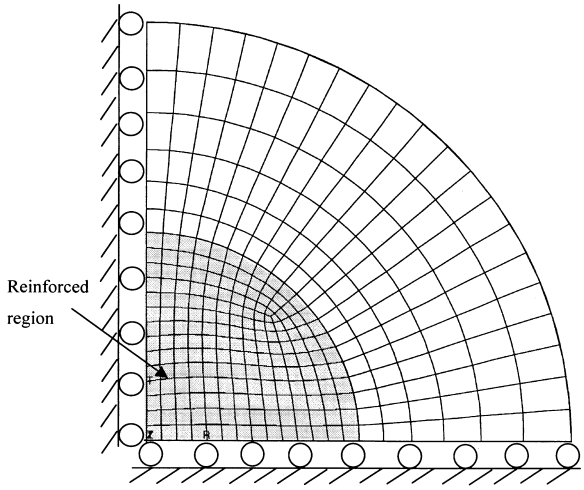

Fig. 6. Finite element mesh of a quarter model.

become

$$\sigma_0^{\mathrm{T}} = \alpha E T_{\mathrm{i}} \frac{(1-\nu_{\mathrm{R}})(1-e/\alpha)+(1-\alpha_{\mathrm{R}}/\alpha)(1+\nu)S\lambda}{(1-\nu_{\mathrm{R}})(1+\lambda+\lambda\nu-\nu)+(1-\nu^2)S\lambda} \tag{78}$$

where $S = E_{\mathrm{R}} t_{\mathrm{R}}/E_{\mathrm{P}} t_{\mathrm{P}}$, and the parameter e is given by Eq. (70). For an infinite patch with $R_{\mathrm{i}}/R_{\mathrm{o}} \to 0$ and $T_{\mathrm{o}} = 0$, one can further show that the residual thermal stress reduces to, noting $\lambda = 1$ and $e = 0$,

$$\sigma_0^{\mathrm{T}} = \alpha E T_{\mathrm{i}} \frac{1-\nu_{\mathrm{R}}+(1-\alpha_{\mathrm{R}}/\alpha)(1+\nu)S}{2(1-\nu_{\mathrm{R}})+(1-\nu^2)S} \tag{79}$$

It is evident that in the special case of isotropic patch, the final solution is dramatically simplified, providing a simple estimate of the residual stress in the plate. It is worth noting that Eq. (79) corrects an error in an earlier solution by Rose (1988). As illustrated in Fig. 9, as far as the stress in the plate is concerned, the isotropic patch assumption does provide a reasonable estimate of the stress in the plate parallel to the fibre direction of the reinforcement. In the context of composite patching, since the fibre direction of the patch is normally aligned perpendicular to the crack being repaired, the x-component of stress is the residual stress of most concern. By contrast, the stresses in the reinforcement are poorly predicted based on the isotropic reinforcement assumption.

To illustrate the influence of the outer boundary of the circular plate on the thermal stresses, Fig. 10 shows the comparison between the theoretical solutions and finite element results of the thermal stresses induced by cooling. When compared with the results with those corresponding to the case clamped edge, there seems to be an even better correlation between the theoretical calculations and the finite element results. Furthermore, the thermal stresses in the plate and the reinforcement increase as the radius of the plate increases, contrary to the case of clamped edge. It is expected that in the limiting case of the radius of the plate being far greater than the patch size, solutions will converge to those corresponding to an infinite plate being reinforced with a circular plate.

Frequently a simple solution has been used in the literature to estimate the thermal residual stress present in a patched specimen employed in laboratory study of composite repairs (Eq. 6.1a, Baker, 1988). In this case the specimen is normally heated and cooled uniformly in an oven during curing. However, in deriving the thermal stress in the plate, the thermal contraction of the region outside the

patch was neglected. Furthermore, by idealising the problem as a one-dimensional one, the lateral constraint present in a real specimen was also ignored. Based on the preceding results, the thermal residual stress pertaining to a patched specimen can be derived, assuming the patch can be idealised as isotropic. This can be achieved by setting $T_o = T_i$, $R_i/R_o \to 0$, and $k = 0$, leading to

$$\lambda = 1, \quad \beta = 1, \quad e = \alpha \tag{80}$$

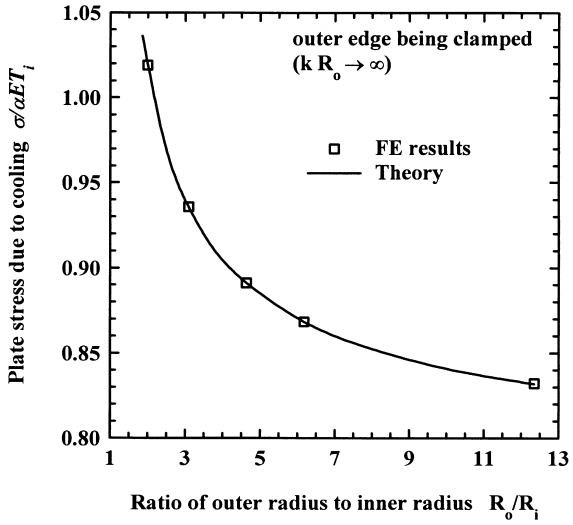

(a)

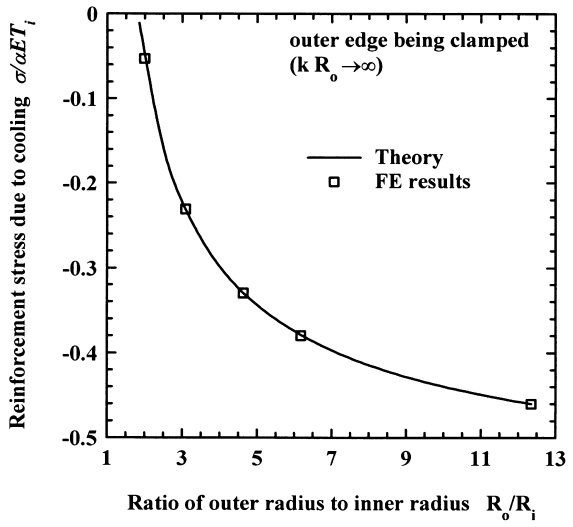

(b)

Fig. 7. Residual thermal stresses for isotropic patch: (a) the plate and (b) the reinforcement.

Consequently, the thermal residual stress upon cooling the specimen from a temperature of T_i to the ambient temperature is

$$\sigma_0^T = \alpha E T_i \frac{(1+\nu)(1-\alpha_R/\alpha)S}{2(1-\nu_R)+(1-\nu_R^2)S} \tag{81}$$

which provides an improved solution for the thermal residual stress in a patched specimen being cured in a uniform temperature field. For a typical balanced repair with $S=1$ and $\nu=\nu_R=0.3$, the above equation yields a thermal stress about 12.6% higher than that reported in the literature (Baker, 1988).

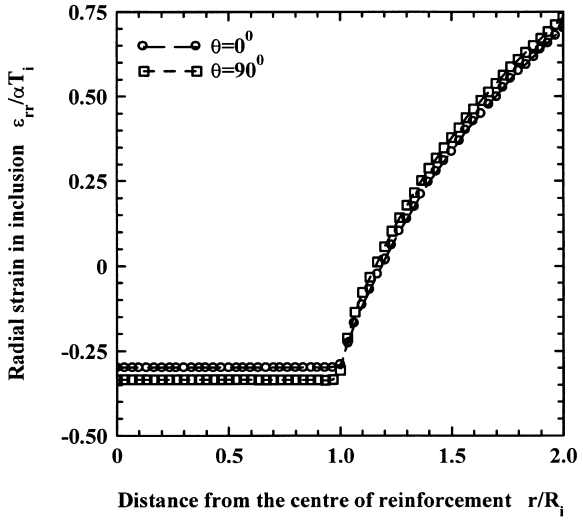

(a)

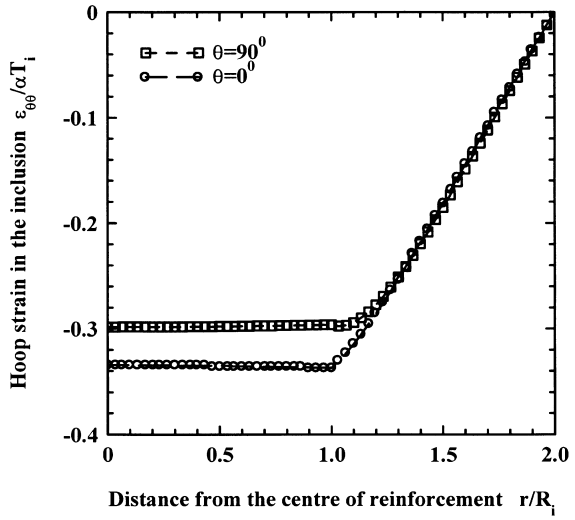

(b)

Fig. 8. Finite size orthotropic patch distributions of (a) the radial strain and (b) the hoop strain.

However, for orthotropic reinforcements, the solutions derived assuming that the patch being isotropic would generally overestimate the thermal residual stress in the plate, as indicated in Fig. 9. Therefore, the thermal stress determined using the present isotropic solution should be regarded as approximate upper bound only.

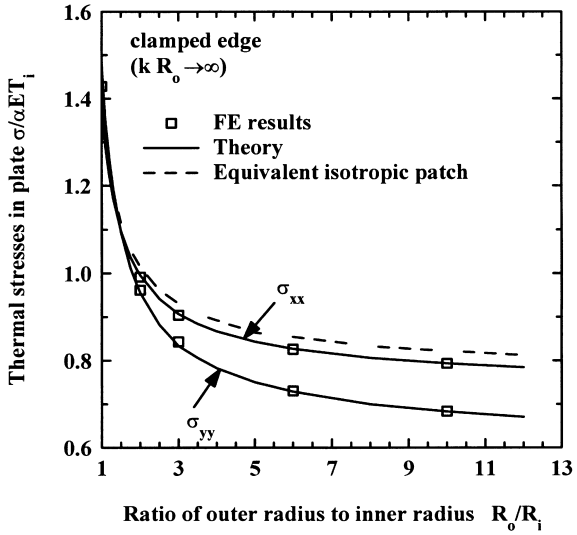

(a)

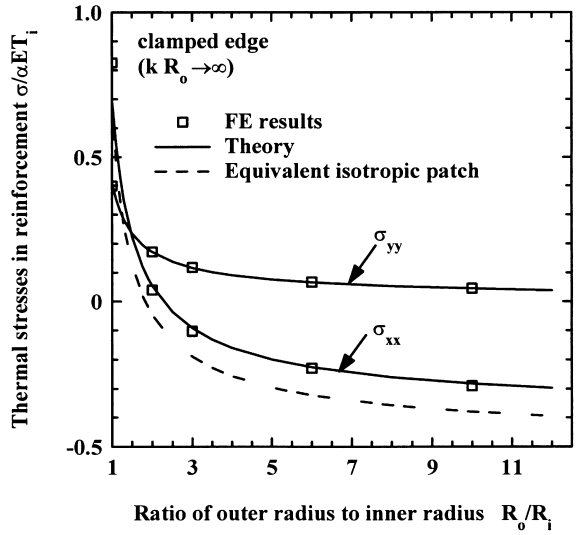

(b)

Fig. 9. A circular patch over a concentric plate with outer edge being clamped; cooling induced stresses in (a) the plate and (b) the orthotropic reinforcement.

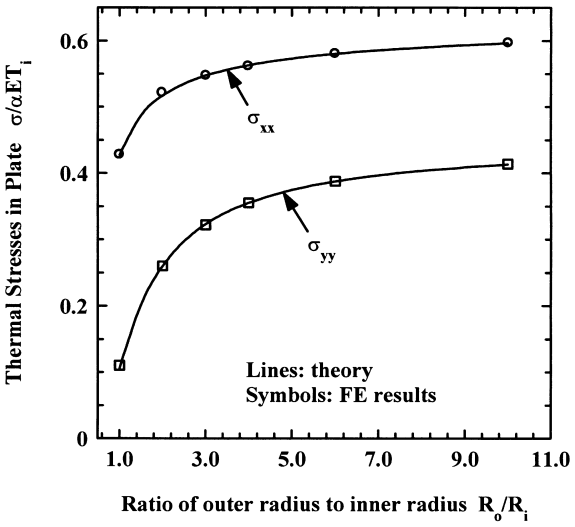

(a)

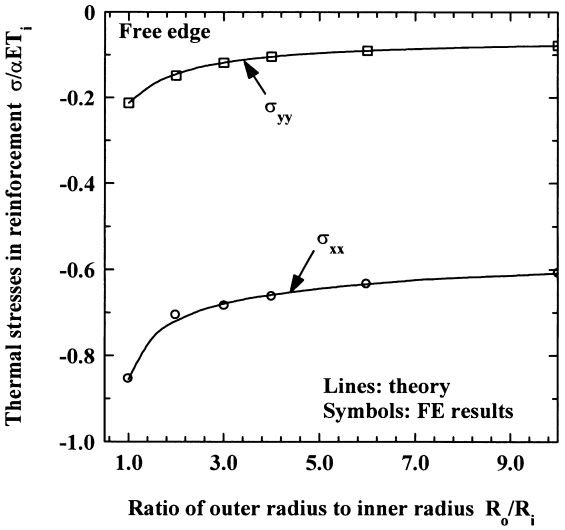

(b)

Fig. 10. A free edge circular plate reinforced with a concentric reinforcement; cooling induced stresses in (a) the plate and (b) the orthotropic reinforcement.

7. Conclusions

Based on an inclusion analogy, an exact solution has been obtained for the thermal stresses in a circular orthotropic composite reinforcement over an infinite isotropic plate. The validity of the analytical solutions has been confirmed by comparisons with finite element results. To quantify the size

effect associated with repairing finite size structures, approximate solutions have also been derived, which are shown to be in close agreement with finite element results. These solutions provide a convenient means for the design and analysis of bonded repairs in relation to the thermal stresses.

References

Baker, A.A., 1988. Crack patching: experimental studies, practical applications. In: Baker, A.A., Jones, R. (Eds.), Bonded Repair of Aircraft Structures. Martinus Nijhoff, Dordrecht, pp. 107–173.

Callinan, R.C., Sanderson, S., Tran-Cong, T., Walker, K., 1997. Development and validation of a finite element based method to determine thermally induced stresses in bonded joint of dissimilar materials. DSTO RR-0109, Aeronautical and Maritime Research Laboratory, Melbourne, Australia.

Eshelby, J.D., 1957. The determination of the elastic field of an ellipsoidal inclusion, and related problems. Proceedings of Royal Society of London A241, 376–396.

Lekhnitskii, S.G., 1963. Theory of Elasticity of an Anisotropic Elastic Body. Holden-Day, San Francisco.

Muskhelishvili, N.I., 1953. Some Basic Problems of the Mathematical Theory of Elasticity. Noordhoff, Leiden.

Rose, L.R.F., 1981. An application of the inclusion analogy for bonded reinforcements. International Journal of Solids and Structures 17, 827–838.

Rose, L.R.F., 1988. Theoretical analysis of crack patching. In: Baker, A.A., Jones, R. (Eds.), Bonded Repair of Aircraft Structures. Martinus Nijhoff, Dordrecht, pp. 77–106.

Timoshenko, S.P., Goodier, J.N., 1970. Theory of Elasticity, 3rd ed. McGraw-Hill, New York.